# Quantitative and realistic description of the magnetic potential energy of spin-torque vortex oscillators

Simon DE WERGIFOSSE,* Chloé CHOPIN, and Flavio ABREU ARAUJO
*Institute of Condensed Matter and Nanosciences, Université catholique de Louvain, Place Croix du Sud 1, 1348 Louvain-la-Neuve, Belgium*

Understanding the dynamics of magnetic vortices emerged as an important challenge regarding the recent development of spin-torque vortex oscillators. Either micromagnetic simulations or analytical Thiele equation approach are typically used to study such system theoretically. This work focuses on the precise description of the restoring forces, due to the different energy terms, exerted on the vortex when it is displaced from equilibrium. In particular, the stiffness parameters related to a modification of the potential magnetic energy terms are investigated. An innovative method is proposed to extract exchange, magnetostatic and Zeeman stiffness expressions from micromagnetic simulations. These expressions, valid up to a never reached before vortex core position, are compared to state-of-the-art analytical results. Furthermore, it is shown that the stiffness parameters depend not only on the vortex core position but also on the injected current density. This phenomenon is not predicted by commonly used analytical ansätze. We foresee that these findings may arise from a deformation of the theoretical magnetic topology caused by the current induced Ampère-Oersted field.

## I. INTRODUCTION

Magnetic vortices are one of the encountered magnetic ground states in soft ferromagnets of reduced dimensions. This non-uniform topology is characterized by curling in-plane spins swirling around a small area called the vortex core, where the magnetization points out-of-plane. Such distribution results from a favorable trade-off between exchange and magnetostatic energies, arising for a wide range of nanodot aspect ratios.[1] Two main topological parameters are typically used to describe a vortex,[2] namely the chirality $C$ and the polarity $P$. On the one hand, the chirality indicates whether the in-plane magnetization curls clockwise ($C = -1$) or counterclockwise ($C = +1$). On the other hand, the polarity informs on the direction of the out-of-plane vortex core profile, which either points upwards ($P = +1$) or downwards ($P = -1$). Due to their great stability, vortices have rapidly gained a lot of attention for prospective applications, notably when combined with spintronics.

Indeed, concomitantly to the advances in vortex dynamics understanding were investigated the first spin-torque nano-oscillators.[3–6] This type of device, based on a magnetic tunnel junction structure, allows to inject a spin-polarized current into a free ferromagnetic layer. As a spin-transfer torque is exerted on its magnetization by conservation of angular momentum, it allows to act on the direction of its mean magnetic moment. By magnetoresistance effects, an alternating signal may thus be retrieved when injecting a constant current into these cylindrical heterostructure. This makes it one of the smallest dc to ac converter. As noted above, it may happen that, for some geometries, the free layer presents a vortex as its magnetic ground state. This led to the development of what are called spin-torque vortex oscillators[7] (STVOs). In the absence of any external excitation, the vortex core is situated at the center of the nanodot. However, if a sufficient input current is applied to the heterostructure and providing conditions on vortex topological parameters,[8] steady-state fluctuations of magnetization may occur. These oscillations, usually in the hundreds of MHz range, are caused by a shift of the moving vortex core towards a nonzero orbit of precession. For very large excitation, the off-centered vortex may even be expelled from the nanodot which can result in a damping due to a polarity switch[9–12] or more exotic magnetic states.[13,14] Besides good stability, STVOs present many advantages,[7] e.g., low noise sensibility, no external field required, narrow bandwidth and wide frequency tunability, which made them a tool of choice for radiofrequency[13] or artificial intelligence applications.[15,16]

As STVOs started to gain interest, theoretical studies on vortex dynamics became crucial to capture and predict device properties such as the frequency or emitted power. Micromagnetic simulations and the so-called Thiele equation[17,18] framework are typically used to examine such systems. Among all aspects of vortex dynamics, the description of restoring forces associated to a displacement of the vortex core from its equilibrium position has been a particularly rich research topic. Stiffness parameters, associated to each potential magnetic energy terms, are commonly defined to characterize the recalling force as it would be done for classical springs. These spring-like parameters have been extensively studied analytically.[2,8,12,19] However very few groups have been able to retrieve them from micromagnetic simulations.[20–22] In this work, expressions valid up to large vortex core position value will be extracted from simulations using an innovative method. We will then compare them to most convincing analytical works from the literature.

## II. METHODS

The Thiele equation approach (TEA) is usually used to describe analytically the dynamics of magnetic vortices confined in the free layer of magnetic tunnel junctions. This theoretical framework allows to predict the vortex core in-plane position $\mathbf{X} = (X, Y)$ by looking at the sum of forces acting on it. The core is thus seen as a quasi-particle representative of any modification of the global magnetic distribution. At equilibrium, the most general way to express this system[2] is given as

$$\mathbf{F}^{\mathrm{M}} + \mathbf{F}^{\mathrm{G}} + \mathbf{F}^{\mathrm{D}} = \mathbf{F}^{\mathrm{R}} + \mathbf{F}^{\mathrm{ext}}, \tag{1}$$

where $\mathbf{F}^{\mathrm{M}}$ is an inertial mass term, $\mathbf{F}^{\mathrm{G}}$ is the gyrotropic force related to the dominant excitation mode of the vortex at low frequency, $\mathbf{F}^{\mathrm{D}}$ is a Gilbert dissipation term, $\mathbf{F}^{\mathrm{R}}$ are the restoring forces and $\mathbf{F}^{\mathrm{ext}}$ represents any additional external forces. For an isolated STVO, the latter are mainly related to spin-transfer torques.[23,24]

Any displacement of the vortex core from its original ground state is associated to a modification of the potential magnetic energy $W$. By analogy to simple harmonic motions, one can define a stiffness $k$ to the system. Keeping all generality, this spring-like parameter is not constant but depends on the degree of deformation, i.e., the vortex core position here. Knowing its value allows to calculate the restoring force appearing in Eq. (1) as

$$\mathbf{F}^{\mathrm{R}} = \frac{\partial W}{\partial \mathbf{X}} = k\mathbf{X}. \tag{2}$$

Neglecting magnetocrystalline anisotropy and any external magnetic field, the potential magnetic energy $W$ is composed of three terms, namely the exchange $W^{\mathrm{ex}}$, magnetostatic $W^{\mathrm{ms}}$ and Zeeman $W^{\mathrm{Z}}$ $(= W^{\mathrm{Oe}})$ energies, the latter being thus only associated to the current induced Ampère-Oersted field (AOF). Based on these hypotheses, the total energy $W$ can be calculated as[12,25]

$$W = \int_V \left( \frac{A}{2}(\nabla \mathbf{m})^2 - \frac{1}{2}\mathbf{M}\cdot\mathbf{H}^{\mathrm{ms}} - \mathbf{M}\cdot\mathbf{H}^{\mathrm{Oe}} \right) dV, \tag{3}$$

where $V$ is the volume of the magnetic dot, $\mathbf{m} = \mathbf{M}/M_{\mathrm{s}}$ is the normalized magnetization, with $M_{\mathrm{s}}$ the saturation magnetization, $A$ is the exchange stiffness coefficient and $\mathbf{H}^{\mathrm{ms}}$ and $\mathbf{H}^{\mathrm{Oe}}$ are the magnetostatic and AO fields, respectively.

To proceed to further calculations from Eq. (3), a mathematical description of the magnetization distribution for a vortex state in circular nanopillars of radius $R$ is required. The most dominant theoretical framework that emerged in the literature, developed by Guslienko *et al.*,[26,27] is the so-called two vortex ansatz (TVA). This model relies on the combination of two off-centered rigid vortices with cores situated in $\mathbf{X} = (\rho, \varphi)$ and $\mathbf{X}_{\mathrm{I}} = (R^2/\rho, \varphi)$, in polar coordinates. Contrary to former descriptions, it presents the advantage of meeting Dirichlet boundary conditions, i.e., no net magnetic charge at the surface edge of the dot. Following TVA, the magnetization at any point $\mathbf{r}$ in the nanodot can be characterized by a planar angle $\phi$ and core profile angle $\Theta$. Those are given as

$$\begin{cases} \phi = \arg(\mathbf{r} - \mathbf{X}) + \arg(\mathbf{r} - \mathbf{X}_{\mathrm{I}}) - \varphi + C\frac{\pi}{2} \\ \Theta = \arccos(P f_z(||\mathbf{r} - \mathbf{X}||)) \end{cases} \tag{4}$$

where $f_z$ is a function describing the vortex core profile. Various propositions of bell-shaped curves have been reported in previous works.[12,28,29] Straightforwardly, one can express the three spatial components of the magnetization $\mathbf{m}$ using these angles as

$$\mathbf{m} = \begin{bmatrix} m_x \\ m_y \\ m_z \end{bmatrix} = \begin{bmatrix} \cos\phi \sin\Theta \\ \sin\phi \sin\Theta \\ \cos\Theta \end{bmatrix}. \tag{5}$$

Using TVA and Eq. (3), developments have been undertaken in the past two decades to obtain expressions of the stiffness parameters $k^{\mathrm{ex}}$, $k^{\mathrm{ms}}$ and $k^{\mathrm{Oe}}$, related to each energy component. The ones valid up to the largest value of the reduced orbit radius $s = ||\mathbf{X}||/R$ from all available in the literature are listed hereafter.

Gaididei *et al.*[12] obtained the following expression for the exchange contribution, based on developments from Guslienko *et al.*,[19]

$$k^{\mathrm{ex}} = (2\pi)^2 h M_{\mathrm{s}}^2 \left(\frac{l_{\mathrm{ex}}}{R}\right)^2 \frac{1}{1-s^2}, \tag{6}$$

where $l_{\mathrm{ex}} = \sqrt{A/(2\pi M_{\mathrm{s}}^2)}$ is the exchange length of the material and $h$ is the thickness of the free layer. Concerning the magnetostatic term, we recently solved[8] the expression of the energy $W^{\mathrm{ms}}$ proposed by Gaididei *et al.*,[12] which led to

$$k_\xi^{\mathrm{ms}} = \frac{8 M_{\mathrm{s}}^2 h^2}{R} \Lambda_{0,\xi} \left(1 + a_\xi s^2 + b_\xi s^4 + c_\xi s^6\right) \tag{7}$$

where $\Lambda_{0,\xi}$, $a_\xi$, $b_\xi$ and $c_\xi$ are coefficients that can be calculated numerically for each value of the nanodot aspect ratio $\xi = h/(2R)$. Finally, we developed in the same study[8] an expression for the contribution associated to the AOF, $\kappa^{\mathrm{Oe}} = k^{\mathrm{Oe}}/(CJ)$, with $J$ being the current density imposed. It is expressed as

$$\kappa^{\mathrm{Oe}} = \frac{8\pi^2}{75} M_{\mathrm{s}} R h \left(1 - \frac{4}{7}s^2 - \frac{1}{7}s^4 - \frac{16}{231}s^6 - \frac{125}{3003}s^8\right). \tag{8}$$

In addition to these analytical works, micromagnetic simulations (MMS) have been extensively used to investigate STVO dynamics. Those rely on the resolution of the Landau-Lifshiftz-Gilbert-Slonczewski[23,30,31] equation to predict numerically the properties of magnetic systems of reduced dimensions. Despite the fact that TEA derives from the LLGS formalism, the latter is based on the use of an effective magnetic field rather than on spring-like constants. Consequently, there is no direct access to

stiffness parameters from micromagnetism. However, as the orbit radius $s$ and the energy components are available within most solvers, one may still extract them by following the procedure described herebelow. As a first step, the energy must be fitted by a chosen expression, as a function of the vortex core position. Then, these functions must be derived according to Eq. (2) to find the corresponding stiffness parameter. This strategy has already been successfully applied in previous studies,[20–22] although for a limited $s$-span.

In our case, the GPU-based solver mumax$^3$ is used to perform micromagnetic simulations.[32] A magnetic tunnel junction presenting a free layer of radius $R = 100$ nm and thickness $h = 10$ nm is studied. The latter is discretized into cells of dimensions $2.5\times2.5\times5$ nm$^3$. Typical material parameters for permalloy are used. The saturation magnetization and exchange stiffness coefficient are $M_\mathrm{s} = 800$ emu/cm$^3$ and $A = 1.07 \cdot 10^{-6}$ erg/cm, respectively. The Gilbert damping constant $\alpha_\mathrm{G}$ is fixed at 0.01 and the spin-current polarization $p_J$ at 0.2. A polarizer presenting a perpendicular direction of magnetization $\mathbf{p} = (p_x, p_y, p_z) = (0, 0, 1)$ is used. The vortex polarity is chosen to be $P = -1$. Current densities of 2, 4, 6 MA/cm$^2$ are imposed into the oscillator, in the positive $z$-direction which allows to respect one of the two necessary conditions for steady-state precessions[8] (i.e., $JPp_z < 0$). The second criterion is to inject a current exceeding the first critical current density $J_{\mathrm{c}1}$. When $J < J_{\mathrm{c}1}$, simulations are initiated with a vortex core translated to $s = 0.9$ and left damping back to the center of the dot, i.e., $s = 0$. For $J > J_{\mathrm{c}1}$ however, two simulations are required to explore the whole range of $s$ for a given current, as the steady-state orbit is different from zero. Each time, the first one is started at $s = 10^{-4}$ and the second one at $s = 0.9$. Both are stopped at steady-state. The influence of temperature is not taken into account in this study. In addition, three different situations are explored, depending on the relative orientation between the in-plane curling magnetization and the AOF. A first set of simulations is performed without considering $\mathbf{H}_\mathrm{Oe}$, then a set with $\mathbf{H}_\mathrm{Oe}$ parallel to the curling magnetization, i.e., $C = +1$, and finally a set with $\mathbf{H}_\mathrm{Oe}$ antiparallel to the curling magnetization, i.e., $C = -1$. Those are labelled below in this manuscript as noOF, $C^+$ and $C^-$, respectively. The vortex core position $s$ as well as the energy components $W^\mathrm{ex}$, $W^\mathrm{ms}$ and $W^\mathrm{Oe}$ are internally computed by mumax$^3$ between each timestep.

The arbitrarily chosen functions for fitting the energy components are even power polynomials of $10^\mathrm{th}$ order, preceded by a pre-factor dependent on material and geometrical parameters. They have the following form

$$W^\mathrm{ex} = -\pi h A \sum_{i=0}^{5} w_i^\mathrm{ex} s^{2i}, \tag{9}$$

$$W^\mathrm{ms} = 4M_\mathrm{s}^2 h^2 R \sum_{i=0}^{5} w_i^\mathrm{ms} s^{2i}, \tag{10}$$

$$W^\mathrm{Oe} = -\frac{\pi}{5} C J M_\mathrm{s} R^3 h \sum_{i=0}^{5} w_i^\mathrm{Oe} s^{2i}. \tag{11}$$

Nonlinear least square fits are performed for $s \in [5 \cdot 10^{-4}, 0.7]$, the upper value being close to the limit of vortex stability.[8] Using an adapted version of Eq. (2), i.e., $k = (\partial W/\partial s)/(sR^2)$, one can easily derive the expressions of the spring-like stiffness parameters, given as

$$k^\mathrm{ex} = -\frac{\pi h A}{R^2} \sum_{i=1}^{5} (2i) w_i^\mathrm{ex} s^{2(i-1)}, \tag{12}$$

$$k^\mathrm{ms} = \frac{4M_\mathrm{s}^2 h^2}{R} \sum_{i=1}^{5} (2i) w_i^\mathrm{ms} s^{2(i-1)}, \tag{13}$$

$$\kappa^\mathrm{Oe} = -\frac{\pi}{5} M_\mathrm{s} R h \sum_{i=1}^{5} (2i) w_i^\mathrm{Oe} s^{2(i-1)}. \tag{14}$$

Let us add that a pre-treatment on micromagnetic results is used before fitting. It consists in ignoring data points too densely packed, followed by an interpolation of the remaining values. It ensures a more homogeneous distribution of the data along the vortex core position axis.

## III. RESULTS & DISCUSSION

Micromagnetic results are compared to the analytical expressions presented previously (see Eq. (6), (7) & (8)). The evolution of the restoring parameters $k^\mathrm{ex}$, $k^\mathrm{ms}$ and $\kappa^\mathrm{Oe}$ with respect to the vortex core position is depicted on Figs. 1, 2 & 3, respectively. Let us start with general observations valid for the three energies. A slight disagreement is noticed between micromagnetism and TEA, even when the vortex core is at the center of the nanodot. These discrepancies could originate from two main hypotheses performed during TEA calculations. Firstly, the out-of-plane magnetization component $m_z$ is neglected for each derivation,[8,12] due to the small area occupied by the vortex core. This simplification, necessary to obtain fully analytical expressions, is applicable as a preliminary approximation. However, even if the vortex core profile contribution is small, it is still different from zero. This is especially true for nanopillars of reduced radius, where the vortex core occupies a non-negligible surface inside the free layer. Secondly, the magnetization $\mathbf{m}$ is considered constant along the dot thickness. Even if appropriate for nanodots presenting a thickness of the order of the exchange length,[1,2,10] this assumption is not

perfectly verified in micromagnetic simulations. In addition, supplementary deviations arise for an off-centered moving vortex core, explaining partly the TEA imperfect modeling when $s$ evolves. Indeed within TVA, the vortex core is simply translated to a greater orbit, while keeping its original shape. Various groups[11,20,22] have already shown the limitations of such theoretical framework to model accurately dynamic vortices. It is also well-known that a vortex core approaching the dot edge see a growing trail of opposite magnetization appearing next to it.[10,12] Such dip, later responsible for the nucleation of a vortex of reversed polarity, surely induces energy changes not perceived within TEA.

Furthermore, a current induced splitting of the stiffness parameters can be observed, as already reported by Choi *et al.*.[21] For increasing currents, the $C^-$ and $C^+$ curves move further apart from the noOe case. This behavior is not predicted at all by TEA calculations. We postulate that these findings result from a modification of the spin distribution $\mathbf{m}$ by the AOF. Spins would be titled under its influence, deviating thus from the theoretical TVA magnetization. This distortion would increase near the dot edges as the AOF amplitude depends linearly on the radial coordinate $r$ inside the free layer. This conclusion is supported by the fact that, in the noOe configuration, the stiffness is independent from the current value. Moreover, the splitting increases with the current density as the AOF amplitude is proportional to the latter. After these preliminary observations, let us now look at each of the confinement contributions in more detail.

The TEA exchange stiffness parameter $k^{\mathrm{ex}}$ is the term presenting the most imprecise description compared to the simulated behavior (see Fig. 1). At low $s$, the analytical value underestimates all MMS. The predicted evolution is satisfying for a slightly off-centered vortex but diverges[12,19] to infinity for $s \to 1$, as expected from Eq. (6). This does not reflect the behavior extracted from simulations as a maximum seems to appear at $s \approx 0.7$ (at least for $C^-$ and noOe), followed by a decrease of the $k^{\mathrm{ex}}$ value. Moreover, a very large impact of the AOF is noticed. For a centered vortex core and $J = 6$ MA/cm$^2$, the exchange stiffness in $C^+$ configuration is 18% larger than the curve of opposite chirality. This value grows up to 31% at $s = 0.7$. Such considerable influence is linked to the fact that the gradient of magnetization $\nabla\mathbf{m}$ appears in the exchange energy formula, as shown in Eq. (3). Any slight deviation in spin directions appearing in simulations with AOF has thus a major impact on the stiffness results compared to calculations using the unaffected theoretical distribution.

As expected the magnetostatic confinement (see Fig. 2) dominates largely both other terms,[2,33] at least for the range of currents explored. For dots with wider radius, or at very large current density, the AOF stiffness parameter $k^{\mathrm{Oe}}$ should gain relative importance. The analytical expression of $k^{\mathrm{ms}}$ overestimates the value extracted from simulations (for the noOe case) by 10% at $s = 0$. This result is consistent with the overvaluation

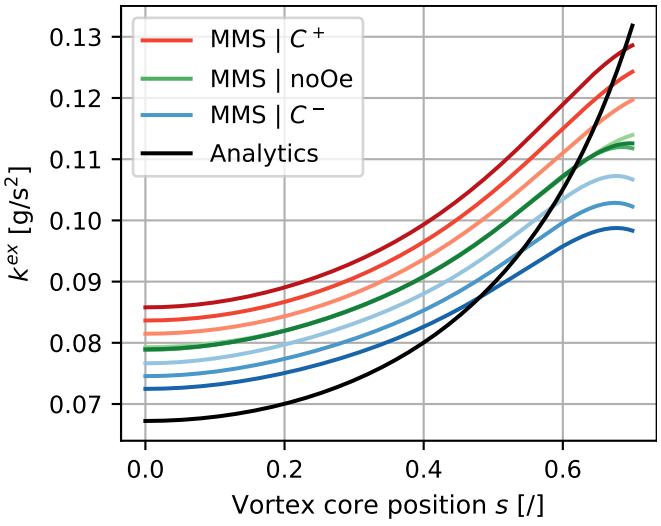


FIG. 1. Exchange stiffness parameter $k^{\mathrm{ex}}$ as a function of the vortex core position $s$. The analytical expression (black line, see Eq. (6)) is compared to micromagnetic simulation (MMS) results (color lines, see Eq. (12)). The colours green, red and blue correspond to simulations without AOF (noOF), with AOF and $C = +1$ ($C^+$) and with AOF and $C = -1$ ($C^-$). The applied current densities $J_{\mathrm{dc}}$ were 2, 4 and 6 MA/cm$^2$, from lighter to darker on the figure. MMS results were obtained after performing a nonlinear least squares fit on the exchange energy (see Eq. (9) & (12)).

of the first critical current $J_{\mathrm{c1}}$ and eigenfrequency $\omega_0$ observed in our previous study[8] when using TEA, as $J_{\mathrm{c1}}$ and $\omega_0 \propto k^{\mathrm{ms}}(s = 0)$. As depicted in Fig. 2, the magnetostatic confinement constantly increases as the core moves towards the edge, for both methods. Though the growth is limited, as $k^{\mathrm{ms}}$ is only 15% greater at $s = 0.7$ compared to the centered vortex case (for noOe). The analytical function models well the simulated evolution of $k^{\mathrm{ms}}$ with respect to $s$ for low vortex displacement. For greater $s$ values however, discrepancies are observed between methods. This difference is partly explained by the moderately high-order polynomial used in Eq. (7). The AOF seems to have a limited impact on the magnetostatic energy, all curves being close to the noOe configuration.

The analytical expression of $\kappa^{\mathrm{Oe}}$ underestimates simulation results (see Fig. 3), for both $C^+$ and $C^-$. However the predicted behavior describes finely its evolution on the whole $s$ range. It may be due to the higher order polynomial used in Eq. (8). More fundamentally, the AOF does not present any out-of-plane component as it appears in a plane perpendicular to the current direction, if edge effects are neglected.[8] Following Eq. (3), the out-of-plane vortex magnetization $m_z$ has thus no impact on the Zeeman energy. Nevertheless, constantly decreasing curves are obtained, $\kappa^{\mathrm{Oe}}$ being 40% greater for a centered vortex than in $s = 0.7$. In addition, a non-negligible impact of the AOF is again perceived on its own stiffness parameters $\kappa^{\mathrm{Oe}}$, in the simulations. This result was ex-

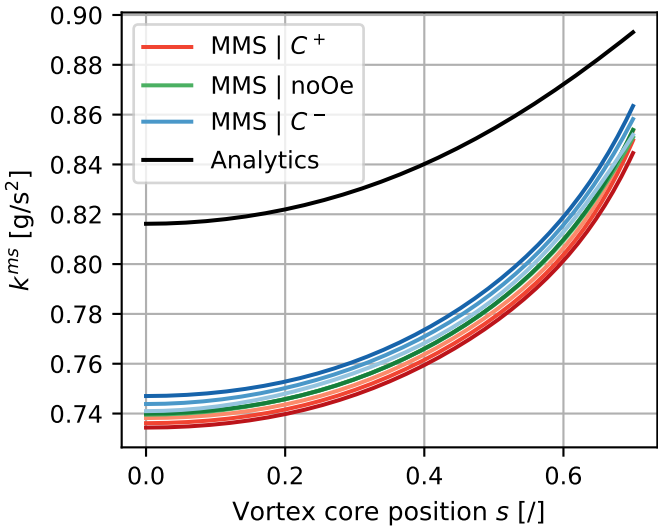


FIG. 2. Magnetostatic stiffness parameter $k^{\mathrm{ms}}$ as a function of the vortex core position $s$. The analytical expression (black line, see Eq. (7)) is compared to micromagnetic simulation (MMS) results (color lines, see Eq. (13)). The colours green, red and blue correspond to simulations without AOF (noOF), with AOF and $C = +1$ ($C^+$) and with AOF and $C = -1$ ($C^-$). The applied current densities $J_{\mathrm{dc}}$ were 2, 4 and 6 MA/cm$^2$, from lighter to darker on the figure. MMS results were obtained after performing a nonlinear least squares fit on the magnetostatic energy (see Eq. (10) & (13)).

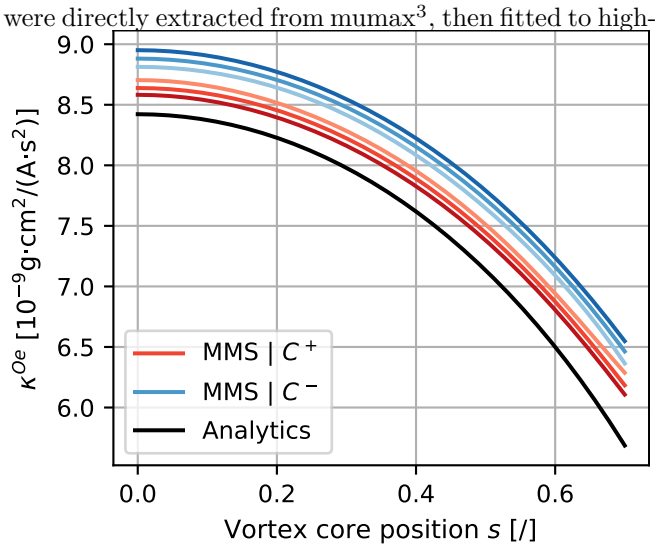


FIG. 3. Ampère-Oersted field (Zeeman-like) stiffness parameter $\kappa^{\mathrm{Oe}}$ as a function of the vortex core position $s$. The analytical expression (black line, see Eq. (8)) is compared to micromagnetic simulation (MMS) results (color lines, see Eq. (14)). The colours red and blue correspond to simulations with AOF and $C = +1$ ($C^+$) and with AOF and $C = -1$ ($C^-$). The applied current densities $J_{\mathrm{dc}}$ were 2, 4 and 6 MA/cm$^2$, from lighter to darker on the figure. MMS results were obtained after performing a nonlinear least squares fit on the Zeeman magnetic energy (see Eq. (11) & (14)).

pected, as we suspect a modification of the magnetization distribution $\mathbf{M}$ appearing in Eq. (3). The splitting stays roughly constant in amplitude, irrespective of the vortex core position.

To put these results into perspective, we believe that our restoring parameter expressions could be integrated into existing TEA models, to replace analytical expressions. Following such a data-driven approach, i.e., deriving $k^{\mathrm{ex}}$, $k^{\mathrm{ms}}$ and $\kappa^{\mathrm{Oe}}$ from limited set of micromagnetic simulations, one could obtain more reliable results from TEA compared to micromagnetism and, by extension, to experimental results. The downside being that these parameters would only be valid for a given geometry and material parameters. Moreover to obtain expressions valid for a continuous range of currents, one should proceed to an interpolation between a few curves selected cleverly, as the splitting increases with $J$. Nevertheless, this constitutes a promising solution for a more accurate analytical model describing STVOs.

## IV. CONCLUSION

Restoring forces appearing in off-centered magnetic vortex state were examined theoretically. Exchange, magnetostatic and Zeeman stiffness parameters were obtained from simulations and compared to state-of-the-art analytical expressions. To do so, the energy components were directly extracted from mumax[3], then fitted to high-order polynomials. The derivatives of these functions allowed to calculate stiffness parameters, analogously to what is done for classical springs under deformation. Discrepancies between Thiele equation approach results and micromagnetism were observed for each term, such as shifts of the curves and disagreeing behavior for large core position value. More importantly, a chirality dependent splitting was observed in the stiffness value, with a deviation depending on the input current intensity. We postulate that this phenomenon is the result of a modification of the spin distribution caused by the current induced Ampère-Oersted field. This hypothesis is supported by the fact that the stiffness was independent of the current imposed when the AOF was not taken into account. Finally, we believe that the expressions we deducted from simulations could be implemented into existing STVO models to better render experimental results.

## ACKNOWLEDGEMENTS

Computational resources have been provided by the Consortium des Équipements de Calcul Intensif (CÉCI), funded by the Fonds de la Recherche Scientifique de Belgique (F.R.S.-FNRS) under Grant No. 2.5020.11 and by the Walloon Region. F.A.A. is a Research Associate of the F.R.S.-FNRS. S.d.W. aknowledges the Walloon Region and UCLouvain for FSR financial support.

* simon.dewergifosse@uclouvain.be


[1] K. L. Metlov and K. Y. Guslienko, Journal of magnetism and magnetic materials **242**, 1015 (2002).

[2] K. Y. Guslienko, Applied Physics Letters **89**, 022510 (2006).

[3] J. Katine, F. Albert, R. Buhrman, E. Myers, and D. Ralph, Physical review letters **84**, 3149 (2000).

[4] S. I. Kiselev, J. Sankey, I. Krivorotov, N. Emley, R. Schoelkopf, R. Buhrman, and D. Ralph, nature **425**, 380 (2003).

[5] A. Slavin and V. Tiberkevich, IEEE Transactions on Magnetics **45**, 1875 (2009).

[6] Z. Zeng, G. Finocchio, and H. Jiang, Nanoscale **5**, 2219 (2013).

[7] V. Pribiag, I. Krivorotov, G. Fuchs, P. Braganca, O. Ozatay, J. Sankey, D. Ralph, and R. Buhrman, Nature physics **3**, 498 (2007).

[8] F. Abreu Araujo, C. Chopin, and S. de Wergifosse, Scientific Reports **12**, 10605 (2022).

[9] K. Yamada, S. Kasai, Y. Nakatani, K. Kobayashi, H. Kohno, A. Thiaville, and T. Ono, Nature materials **6**, 270 (2007).

[10] K. Y. Guslienko, K.-S. Lee, and S.-K. Kim, Physical review letters **100**, 027203 (2008).

[11] A. Khvalkovskiy, J. Grollier, A. Dussaux, K. A. Zvezdin, and V. Cros, Physical Review B **80**, 140401 (2009).

[12] Y. Gaididei, V. P. Kravchuk, and D. D. Sheka, International Journal of Quantum Chemistry **110**, 83 (2010).

[13] A. Jenkins, R. Lebrun, E. Grimaldi, S. Tsunegi, P. Bortolotti, H. Kubota, K. Yakushiji, A. Fukushima, G. De Loubens, O. Klein, *et al.*, Nature nanotechnology **11**, 360 (2016).

[14] S. Wittrock, P. Talatchian, M. Romera, S. Menshawy, M. Jotta Garcia, M.-C. Cyrille, R. Ferreira, R. Lebrun, P. Bortolotti, U. Ebels, *et al.*, Applied Physics Letters **118**, 012404 (2021).

[15] J. Torrejon, M. Riou, F. Abreu Araujo, S. Tsunegi, G. Khalsa, D. Querlioz, P. Bortolotti, V. Cros, K. Yakushiji, A. Fukushima, *et al.*, Nature **547**, 428 (2017).

[16] M. Romera, P. Talatchian, S. Tsunegi, F. Abreu Araujo, V. Cros, P. Bortolotti, J. Trastoy, K. Yakushiji, A. Fukushima, H. Kubota, S. Yuasa, M. Ernoult, D. Vodenicarevic, T. Hirtzlin, N. Locatelli, D. Querlioz, and J. Grollier, Nature **563**, 230 (2018).

[17] A. Thiele, Physical Review Letters **30**, 230 (1973).

[18] A. Thiele, Journal of Applied Physics **45**, 377 (1974).

[19] K. Y. Guslienko, V. Novosad, Y. Otani, H. Shima, and K. Fukamichi, Applied Physics Letters **78**, 3848 (2001).

[20] K. S. Buchanan, P. E. Roy, M. Grimsditch, F. Y. Fradin, K. Y. Guslienko, S. D. Bader, and V. Novosad, Physical Review B **74**, 064404 (2006).

[21] Y.-S. Choi, S.-K. Kim, K.-S. Lee, and Y.-S. Yu, Applied Physics Letters **93**, 182508 (2008).

[22] J. P. Fried and P. J. Metaxas, Physical Review B **93**, 064422 (2016).

[23] J. C. Slonczewski, Journal of Magnetism and Magnetic Materials **159**, L1 (1996).

[24] Z. Li and S. Zhang, Physical Review B **68**, 024404 (2003).

[25] K. Y. Guslienko, V. Novosad, Y. Otani, H. Shima, and K. Fukamichi, Physical Review B **65**, 024414 (2001).

[26] K. Y. Guslienko and K. L. Metlov, Physical Review B **63**, 100403 (2001).

[27] K. Y. Guslienko, B. Ivanov, V. Novosad, Y. Otani, H. Shima, and K. Fukamichi, Journal of Applied Physics **91**, 8037 (2002).

[28] N. Usov and S. Peschany, Journal of Magnetism and Magnetic Materials **118**, L290 (1993).

[29] R. Hoellinger, A. Killinger, and U. Krey, Journal of magnetism and magnetic materials **261**, 178 (2003).

[30] L. Landau and E. Lifshitz, in *Perspectives in Theoretical Physics* (Elsevier, 1992) pp. 51–65.

[31] T. L. Gilbert, IEEE transactions on magnetics **40**, 3443 (2004).

[32] A. Vansteenkiste, J. Leliaert, M. Dvornik, M. Helsen, F. Garcia-Sanchez, and B. Van Waeyenberge, AIP advances **4**, 107133 (2014).

[33] K. Y. Guslienko, X. Han, D. Keavney, R. Divan, and S. Bader, Physical review letters **96**, 067205 (2006).